NJC

ROYAL SOCIETY OF CHEMISTRY

PAPER

View Article Online
View Journal | View Issue

Cite this: *New J. Chem.*, 2025, **49**, 19570

Acetylation of anilines, amines, and alcohols using 5%MoO_3–SiO_2 and 5%WO_3–ZrO_2 as mesoporous acid catalysts

Nomathamsanqa Prudence Maqunga, Matumuene Joe Ndolomingo, Ndzondelelo Bingwa and Reinout Meijboom *

Received 14th July 2025,
Accepted 23rd October 2025

DOI: 10.1039/d5nj02857d

rsc.li/njc

This paper presents an efficient approach for acetylating anilines, amines and alcohols with acetic anhydride using in-house synthesized and environmentally friendly 5%MoO_3–SiO_2 and 5%WO_3–ZrO_2 acid catalysts. By incorporating molybdenum and tungsten oxides into the porous supports of SiO_2 and ZrO_2, we created acid catalysts with large surface areas that demonstrated excellent reactivity and stability. The 5%MoO_3–SiO_2 catalyst was slightly more active in the acetylation of anilines, with conversions ranging from 76 to 100%. The 5%WO_3–ZrO_2 was more active in the acetylation of alcohols, with conversions ranging from 27 to 99%. The higher surface area of the catalysts and the high nucleophilicity of the amines and anilines appear to be the driving force for higher catalytic activity in these compounds with the HPMC/H_2O system.

1. Introduction

Acetylation plays a crucial role in chemical synthesis. It attaches acetyl groups, which act as shields, protecting various functional groups.[1,2] Chemical molecules frequently contain vulnerable hydroxyl and amino groups, alcohols, anilines and amines. Protecting these areas is crucial during organic processes to prevent unwanted reactions and ensure selective transformations.[1,2] Hydroxyl and amino groups are highly reactive and therefore susceptible to various reactions. Thus, safeguarding or temporarily masking these groups prevents them from interfering with the desired reactions and allows for selective reaction of other functional groups while leaving the protected group intact. Scientists often have to mask the reactivity of hydroxyl and amino groups to perform selective manipulation of other functional groups in the molecule. This allows them to control the overall chemical process and achieve the desired products. The stability of the products in an acidic medium and the ease of adding and removing the acetyl group make it an effective method. Acetylation with acetic anhydride or acetyl chloride in the presence of an acidic or basic catalyst has therefore, proven to be an efficient and widely used approach for protecting hydroxyl and amino groups.[3–5]

The *N*-acylation of amines and, particularly, anilines to the corresponding acetamides has widespread applications in the polymer, agrochemical and pharmaceutical industries.[6] One example in the pharmaceutical industry is the synthesis of acetaminophen (paracetamol) by the acetylation of 4-hydroxyaniline, a drug used to treat pain and fever. Acetylation, the process of adding an acetyl group, is used extensively in various industries to create esters from alcohols. These esters are vital in producing fine chemicals, food preservatives and flavourings, perfumes, plasticizers for polymers, and pharmaceutical products.[7–10] For example, acetylating salicylic acid produces aspirin, a common pain-relief medication.

For this transformation, a variety of catalytic systems are available, but most of them are homogeneous and non-recoverable, and they often have drawbacks such as slow reaction rates, low yields, hazardous conditions, the use of harmful solvents, tedious workup procedures, the use of excess amounts of reagents, and toxic catalysts.[11] Considering the importance of environmental health in chemical technology, it is crucial to diminish the generation of unwanted hazardous and dangerous by-products.[12] As a result, a new, more economically viable catalytic technique that employs milder conditions remains a priority.[4]

The creation of simple, economical, broadly applicable and environmentally friendly procedures is still an active topic of research from a practical standpoint. Solid acids have attracted the interest of researchers from both industry and academia. Synthesizing novel ordered mesoporous structures with pores of various sizes and shapes is particularly compelling.[1] More recently, studies have shown that molybdenum or tungsten-doped zirconia is an effective alternate catalyst for acid–site

Department of Chemical Sciences, University of Johannesburg, Auckland Park, Johannesburg 2006, PO Box 524, South Africa. E-mail: rmeijboom@uj.ac.za; Fax: +27 (0)11 559 2819; Tel: +27 (0)11 559 2367

reactions.[13,14] The goal of this research is to use efficient molybdenum or tungsten-doped solid acid catalysts to acetylate alcohols, amines, and anilines using mild reaction conditions.

It is well known that solvents critically affect the equilibrium and reaction rates in typical organic reactions,[15] and acetylation reactions are often performed in organic solvents. Compared to organic solvents, water is safe and cheap, and is also known to enhance the reaction rates and selectivity of a variety of organic reactions.[16] However, in water, organic reactions are often complex because most organic reactants are insoluble in water. To overcome the solubility problem, surfactants can be used, as they form micelles and promote reactions in water, by leveraging their hydrophobic and hydrophilic groups.[17] The hydroxypropyl methylcellulose (HPMC), a cellulose additive which is not a surfactant but adopts the behaviour of a surfactant, can be used to enhance the solubility and reactivity of organic compounds in water. The HPMC serves as a polymeric solubilizer that uses alkyl ether side chains and the cyclic ether rings to make hydrophobic pockets which then acts as nanoreactors for reaction to occur in them.[18] HPMC enhances the viscosity of an aqueous medium, and 2 wt% HPMC solution was reported as the most suitable.[18,19] Braje *et al.* have reported several organic reactions using this compound in a patent filed in 2017.[19] HPMC is particularly useful for acetylation reactions, which are often performed in organic solvents. By forming hydrophobic pockets in water, it enhances the solubility and reactivity of organic compounds, resulting in faster reaction times in aqueous solutions.[18,20,21] In the context of green and sustainable chemistry, the ability of HPMC to form hydrophobic pockets in water makes it a valuable tool in facilitating and improving the efficiency of acetylation reactions in aqueous media.

2. Materials and methods

2.1. Chemicals

Ammonium metatungstate hydrate (≥99.0%), tetraethyl orthosilicate (≥99.0%), zirconium(IV) oxynitrate hydrate (99%), 4-nitroaniline (98%), ammonium molybdate tetrahydrate (98%), 2-hydroxyaniline (99%), *o*-toluidine (98%), 4-bromoaniline (97%), aniline (97%), 4-hydroxyaniline (≥98%), 1-naphthylamine (99%), cyclohexylamine (≥99.9%), *N*-methylbenzylamine (97%), salicylic acid (99%), benzyl alcohol (99.8%), iso-butanol (99%), 3.3-dimethylbutan-2-ol (97%), cinnamyl alcohol (97%), 1-phenylethanol (98%), 2-phenylethanol (≥99.0%), phenol (≥99%), 1-pentanol (≥99%), isoamyl alcohol (≥98%), ethyl acetate (≥99.5%), decane (≥99%), nitric acid (70%), poly(ethylene glycol)-*block*-poly(propylene glycol)-*block*-poly(ethylene glycol) (Pluronic-P123) (99%) and hydroxypropyl methylcellulose (HPMC) (98%) were all purchased from Sigma Aldrich. Acetic anhydride (97%) was purchased from UniLAB. Butanol (99.5%) was purchased from Rochelle Chemicals. 4-Chloroaniline (99%) and pentan-2-ol (95%) were purchased from BDH Chemicals Ltd, Poole, England. All chemicals were used as received. The deionized water was obtained from an in-house Milli-Q system (18.2 MΩ cm).

2.2. Synthesis of mesoporous materials

A sol–gel approach was used to synthesize the solid mesoporous metal oxide catalysts, adapted from Hlatswayo *et al.*.[13,14] The 5%MoO_3–SiO_2 sample was prepared by weighing approximately 12.4 g of Pluronic-P123 and mixing it with 22.2 mL tetraethyl orthosilicate, 70.4 mL butanol, and 12.6 mL nitric acid (70%). The reagents were thoroughly mixed until it became clear. Then, in a separate beaker, 6.1 g ammonium molybdate tetrahydrate was dissolved in 12.5 mL H_2O and 12.50 mL ethanol, which was gently agitated until clear. The two solutions were then mixed and agitated at room temperature for 20 min. This mixture was baked for six hours at 120 °C before being calcined for one hour at 600 °C under air. The fragile material was washed in ethanol and dried at 60 °C overnight before being grounded into fine particles. Similarly, 5%WO_3–ZrO_2 was made by weighing approximately 12.4 g of Pluronic-P123 and mixing it with 23.1 g zirconium(IV) oxinitrate hydrate, 70.4 mL butanol, and 12.6 mL nitric acid. This mixture was blended until it became clear. In addition, 14.78 g ammonium metatungstate was weighed and dissolved in a solution of 12.5 mL H_2O and 12.5 mL ethanol in a separate beaker, which was similarly agitated until clear. The two solutions were combined and agitated at room temperature for 20 min. It was then baked for six hours at 120 °C before being calcined for one hour at 600 °C under air. The material was rinsed with ethanol and dried at 60 °C overnight before being ground into fine particles.

2.3. Instrumentation and catalyst characterization

Nitrogen sorption measurements on a micromeritics ASAP 2460 sorption system utilizing the Brunauer–Emmett–Teller (BET) method were used to determine the texture of the catalysts, including pore volume, average pore diameter, and surface area. Before the analysis, the samples were degassed with nitrogen gas at 90 °C for 18 hours. An X-ray powder diffraction (p-XRD) pattern was created at room temperature using a Rigaku MiniFlex-600 diffractometer with Cu K-α_1 radiation (λ = 0.1541 nm). Diffraction patterns were measured at a step rate of 0.015° min^{-1} and 0.1° min^{-1} for low angle (2θ = 0–10°) and wide-angle (2θ = 10–80°), respectively, and Match 2! Software was used to analyse the crystalline phases of the catalysts. The morphology of the sample was further investigated using a JEOL-JEM-2100F transmission electron microscope (TEM) with a 200 kV accelerating voltage. For that purpose, the samples were dispersed in ethanol, and a drop was deposited on a carbon-coated copper grid, dried at room temperature, and measured on the device. The materials' surface morphology and elemental mapping were investigated using a VEGA 3 TESCAN scanning electron microscope (SEM) and a 20 kV Oxford energy dispersive X-ray analysis system. Before analysis, the materials were carbon-coated using an Agar Turbo Carbon Coater. The acid sites of the as-synthesized catalysts were verified by temperature programmed desorption method (NH_3-TPD) using a Chemisorption Analyzer Micromeritics AutoChem II 2920. The analysis was performed under a flow ratio of 10 : 90 NH_3-He with a temperature ramping rate of 10 °C min^{-1} from 25 °C to 900 °C.

2.4. General procedure for acetylation

First, a 2% HPMC solution was prepared by heating Millipore water (60 mL) to 70 °C while stirring. Then, 2 g of HPMC was added and stirred until dissolved. Finally, 40 mL of Millipore water was added, and the mixture was allowed to cool to room temperature. Subsequently, 5 mL of the 2 wt% HPMC solution was added to a carousel tube. The substrate in question (1 equiv., 2 mmol), acetic anhydride (2 equiv., 4 mmol), and a catalyst (0.002 equiv.) were then added. The mixture was heated under continuous stirring for 6 hours at 80 °C. Three aliquots of 5 mL ethyl acetate were used to extract the reaction mixture. Magnesium sulphate was used to dry the reaction mixture, after which a silica gel packed column was used to purify it.

2.5. Product analysis

For quantitative analysis, a Shimadzu GC-2010 equipped with a flame ionization detector (FID) and a Restek–800–356–1688 capillary column (30 m × 0.25 mm × 0.25 μm) was used, with injection port and FID temperatures of 250 °C and 300 °C, respectively. The conversion of the substrates, with decane as the internal standard, was monitored using the integrations obtained from the GC-FID data as shown in eqn (S1). The selectivity and the product yields were calculated using eqn (S2) and (S3), respectively. A GC-MS equipped with a capillary column and mass spectrometer was used to confirm the targeted products. The structures of the products were matched from the GC software library. Furthermore, nuclear magnetic resonance spectroscopy (NMR) was used to qualify the reaction products. The ^{1}H NMR (500 MHz) and ^{13}C NMR (125 MHz) spectra were acquired from a Bruker-500 MHz NMR spectrometer, using tetramethylsilane (0.0) as the internal standard.

3. Results and discussion

3.1. Catalyst characterization

Nitrogen sorption studies were used to examine the surface texture of the synthesized catalysts and their respective supports. The results are presented in Fig. 1 and Table 1. The N_2-sorption of all the synthesized materials is displayed in Fig. 1(a). The BET isotherms of the 5%MoO_3–SiO_2 and 5%WO_3–ZrO_2 catalysts and their corresponding metal oxide supports are classified as type IV and demonstrate type H_2 hysteresis, which indicates a mesoporous nature of the materials. The measured BET surface area of the SiO_2 support, as revealed in Table 1, was noticeably higher (590.4 m^2 g^{-1}) than that of the other synthesized materials (<100 m^2 g^{-1}). The high specific surface area of SiO_2 could be related to the presence of a relatively high amount of mesopores as well as microspores within the silica structure. The modification of the silica support with molybdenum resulted in a drastic reduction in the silica support's surface area by 6.1 times. This could be due to the blockage of most of the small pores of silica by the molybdenum particles during the synthesis of the MoO_3–SiO_2 catalyst.

Furthermore, it was also noticed that the surface area of the tungsten-modified ZrO_2 catalyst (62.33 m^2 g^{-1}) was less than that of the ZrO_2 support (86.82 m^2 g^{-1}). This indicated that the doping process was successful because the surface mesostructure of the respective supports (SiO_2 and ZrO_2) was reduced upon the doping process. It was previously reported that doping with a transition metal influences the structural feature and catalytic efficiency of the resulting mixed mesoporous material.[22–24] As expected, the pore diameters in all the synthesized materials are in the mesoporous range, and the surface area of the corresponding materials decreases with an increase in pore diameter. When compared to the SiO_2 support, the 5%MoO_3–SiO_2 sample showed a pore volume decrease to 0.320 cm^3 g^{-1} from 0.546 cm^3 g^{-1}. This can be explained by the amorphous nature of the SiO_2 support, as revealed by the XRD analysis and the plausible blockage of its small pores during the synthesis of the MoO_3–SiO_2 catalyst. In contrast, the 5%WO_3–ZrO_3 showed a pore volume increase (0.212 cm^3 g^{-1}) in comparison to its corresponding support (0.085 cm^3 g^{-1}). This can be due to the dopant causing smaller particles to form, which then leads to more interconnected pores. The effect of dopants on pore volume is context dependent. It was reported that the effect of doping on the pore volume of metal oxides can either increase or decrease, depending on several factors, including the dopant type and the specific metal oxide.[25,26] Different dopants will interact differently with the metal oxide, and different metal oxides can have different effects. The initial porosity and structure of the metal oxide itself will influence

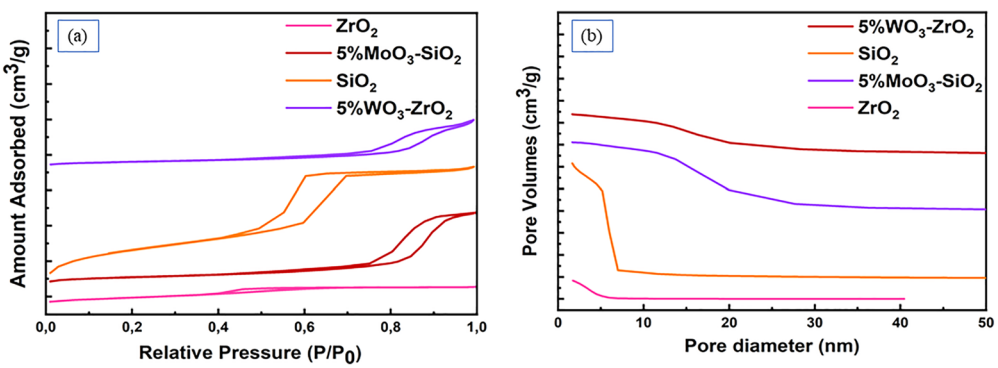

Fig. 1 (a) BET isotherms and (b) pore size distribution plots of the mesoporous metal oxide supports and their respective dopant catalysts.

Table 1 Physisorption a data of the mesoporous metal oxide supports and their respective dopant catalysts

Samples	BET surface area ($m^2\ g^{-1}$)	Pore volume ($cm^3\ g^{-1}$)	Pore diameter (nm)	Acidity (mmol g^{-1})
SiO_2	590.4	0.546	4.656	—
$5\%MoO_3$–SiO_2	97.07	0.320	11.03	0.515
ZrO_2	86.82	0.085	3.143	—
$5\%WO_3$–ZrO_2	62.33	0.212	11.06	0.963

how it responds to doping. Generally, a slight decrease in pore volume can occur if the dopant covers or blocks the existing pores, while an increase is sometimes observed if the dopant causes smaller particles to form, creating new pores.[25,26] Overall, the two catalysts have similar pore diameters; the difference is in their pore volume and surface area, with the $5\%WO_3$–ZrO_3 having smaller pore volumes and surface area.

Fig. 2 depicts the low-angle and wide-angle X-ray diffraction patterns of the two catalysts and their respective metal oxide supports. Specifically, Fig. 2 (b) shows the XRD profile of SiO_2 in the 2θ range from 16° to 30°, revealing a typical broad silica peak indicating the amorphous nature of the material. However, the XRD profile of $5\%MoO_3$–SiO_2 shows intense molybdenum diffractions with sharp narrow peaks indicating that the material is crystalline. This XRD pattern data is consistent with the work reported by Hlatswayo *et al.*[13] and Lin *et al.*[27] The XRD profile of ZrO_2 displayed amorphous peaks, and indicated a match on the Match 2! software (JPCD file 96–500–0039). The synthesized material has a cubic crystal system, with the space group of $Fm\bar{3}m$, an observation also supported by Akinnawo *et al.*[28] The XRD profile of $5\%WO_3$–ZrO_2 has broader peaks than the ZrO_2 support, indicating the amorphous nature of the material. The intensity of the ZrO_2 peaks is also reduced significantly in this profile, which is in line with the literature.[29–31] It was reported that the intensity of ZrO_2 peaks in a WO_3–ZrO_2 profile can be reduced due to the formation of a tungsten-zirconia solid solution, where tungsten atoms migrate into the zirconia lattice, disrupting its structure, altering the unit cell dimensions and symmetry, which leads to less ordered, or even amorphous, ZrO_2. This structural change reduces the crystallinity of the ZrO_2, and consequently, its ability to diffract X-rays, leading to weaker diffraction peaks.[29–31]

Furthermore, there are additional intense peaks due to the tungsten diffractions in the 2θ range from 20° to 25°.[32] There was no significant match on the JCPDS for this profile. However, the findings align with the results reported by Hlatswayo *et al.*[13] and Poyraz *et al.*[32] The catalysts and their respective metal oxide supports showed an amorphous diffraction pattern at low angles below $2\theta = 4°$, indicating a mesoporous nature of the material, except for the $5\%WO_3$–ZrO_2, indicating that the $5\%MoO_3$–SiO_2 had long-range order with regular pore distribution.

The porosity of both catalysts is seen in the representative TEM micrographs (see Fig. 3), with the respective metal clusters shown as black spots in each case. The $5\%WO_3$–ZrO_2 sample is mostly made up of big crystalline particle materials with no discernible form. However, the $5\%MoO_3$–SiO_2 sample was a crystalline combination of large and tiny particulates. These TEM images also illustrated a clear indication of the presence of pores and provided some insights into the material's mesopore structural features.

Fig. 4(a) displays the SEM micrograph of $5\%WO_3$–ZrO_2, which shows the porous texture of the material with large particles and a rough surface. There is no apparent order or shape in these large particles, and this is consistent with what was observed for TEM analysis. The energy-dispersive X-ray analysis (Fig. 4(b)) and elemental mapping (Fig. 4(c–f)) indicate the homogeneity and high purity of the sample with only tungsten, oxygen and zirconium detected in the sample. The same observation is made for the $5\%MoO_3$–SiO_2 sample, as shown in Fig. 5(a), where the micrograph shows the porous texture of the material with a rough sponge-like surface. This result is also in agreement with the TEM result reported above, as there is a combination of large and small particles with no

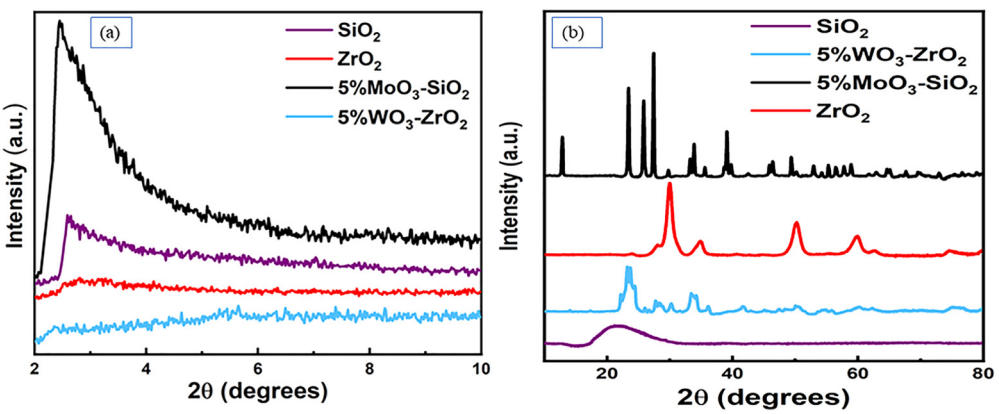

Fig. 2 p-XRD patterns of the mesoporous metal oxide supports and their respective dopant catalysts; (a) low-angle and (b) wide-angle.

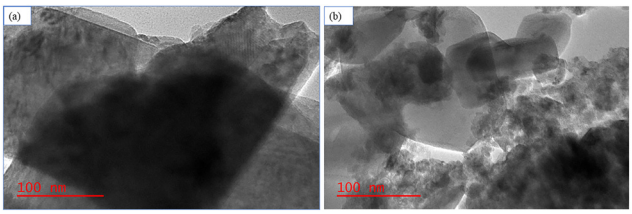

Fig. 3 TEM images of (a) 5%WO_3–ZrO_2 and (b) 5%MoO_3–SiO_2.

apparent order or shape. Also, in Fig. 5(b), the energy-dispersive X-ray analysis and elemental mapping (Fig. 5(c–f)) indicate the homogeneity and high purity of the sample with only molybdenum, silicon and oxygen detected in the sample.

The surface acid properties of the as-synthesized catalysts were investigated by NH_3-TPD. The results are summarised in Table 1. Generally, NH_3-TPD is an extensively utilized method for studying the surface acidity of mesoporous metal oxides.[13,14,33] The acidic strength of the materials is determined by the intensity/area and the position of the NH_3 desorption peaks; the higher the intensity/area, the higher the acidic strength of the material. Weaker acidic sites lie around 200 °C, and acidic sites of strong strength lie above 400 °C.[13,14,34]

As previously reported[13,14] and depicted in Fig. S1, the NH_3-TPD results illustrated that tungsten binds more strongly with NH_3 and this resulted in higher NH_3 desorption temperature and peak intensity/area. Thus, 5%WO_3–ZrO_2 showed an acidity value of 0.963 mmol g^{-1}, indicating a higher acidity content compared to 5%MoO_3–SiO_2 with an acidity value of 0.515 mmol g^{-1}. This observation is not surprising because the tungsten cation is considered a stronger acid than the molybdenum cation. Tungsten's higher acid strength is attributed to its ability to form more stable and strongly bonding interactions with electron-rich species, and is more effective in most catalytic reactions.[35,36] In addition, zirconia is generally a stronger acid than silica; zirconia has a polar surface with zirconium atoms acting as strong acid sites, and silica, while exhibiting some acidity, is normally weaker.[37]

3.2. Catalytic activity studies

Tungsten-modified zirconia (5%WO_3–ZrO_2) and molybdenum-modified silica (5%MoO_3–SiO_2) are the two mesoporous acid catalysts used for the acetylation of anilines, amines, and alcohols. One of the goals was to create a sustainable synthetic method for acetylation of diverse functional groups that was both environmentally benign and energy efficient. As a result, a portion of the experimental design focused on moderate temperature synthesis, as this has both economic and safety implications. For example, a synthetic chemical protocol operating at high temperatures has a higher energy demand and is less sustainable due to the environmental impact of such a demand, not to mention the cost. Secondly, higher temperature experiments constitute a significant safety issue because dangerous explosions and spillages are always a possibility. Moreover, the reaction is catalytic and takes place at a moderate temperature.

It is worth mentioning that, without any catalyst, the acetylation of selected anilines, amines and alcohols with acetic anhydride did not substantially proceed in the time frame of the experiments. The anilines and amines showed less than 15% conversion, while the alcohols showed less than 10%. Nevertheless, when catalysts were used (Tables 2–4), reactions occurred to a significant extent. This observation shows the crucial catalytic role played by the mesoporous acid catalysts in the acetylation process as conducted in this study.

3.2.1. Acetylation of anilines. Anilines are often less nucleophilic than secondary and primary amines, requiring harsher reaction conditions for reactivity.[38] A variety of substituted anilines were evaluated for acetylation to their corresponding acetamide derivatives (Table 2), and in particular, 4-hydroxyaniline as the corresponding acetamide derivative (entry 1) called

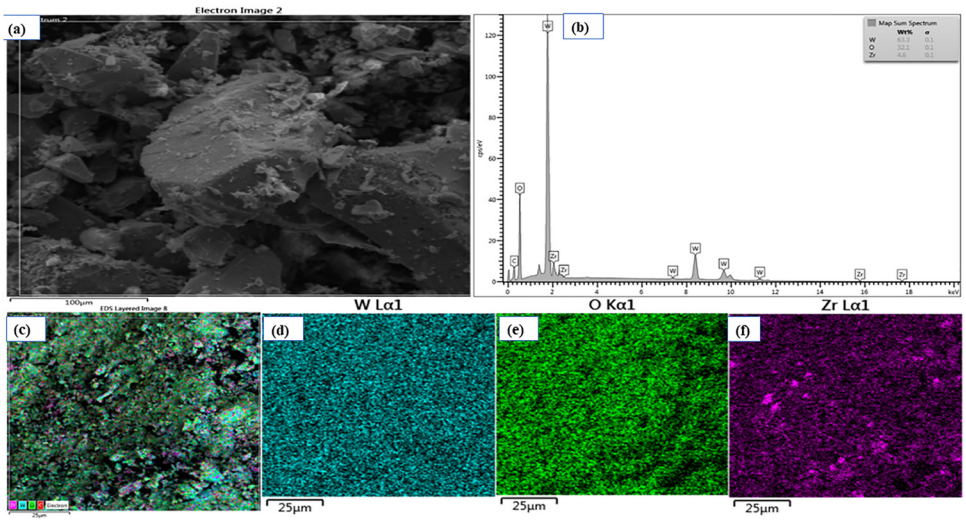

Fig. 4 (a) SEM image, (b) SEM-EDS spectra and (c) elemental mapping of 5%WO_3–ZrO_2; elemental maps of individual constituents of 5%WO_3–ZrO_2, (d) Tungsten, (e) oxygen and (f) zirconium.

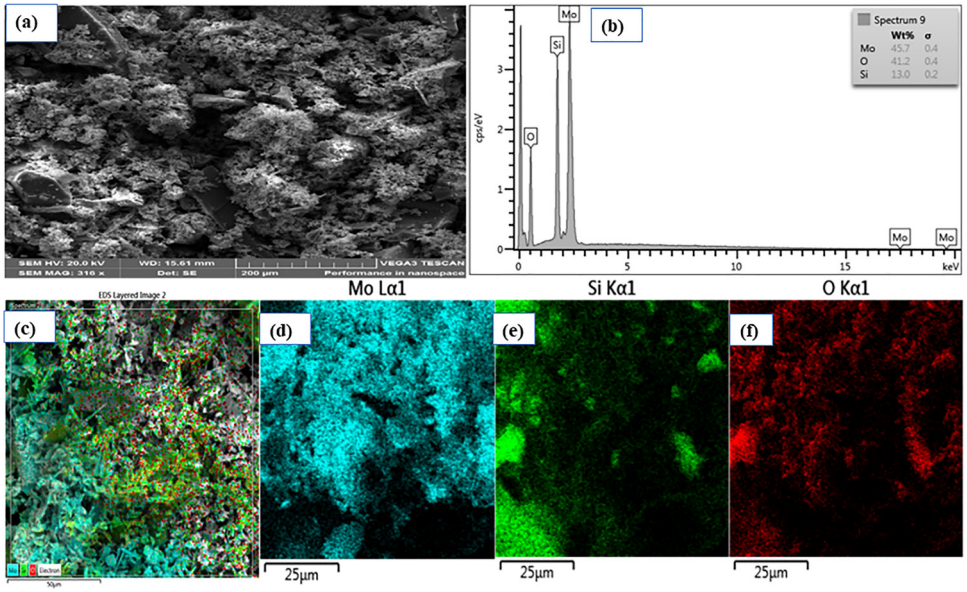

Fig. 5 (a) SEM image, (b) SEM-EDS spectra and (c) elemental mapping of 5%MoO_3–SiO_2; elemental maps of individual constituents of 5%MoO_3–SiO_2, (d) molybdenum, (e) silicon and (f) oxygen.

Table 2 The yields and selectivity of products obtained from the acetylation of selected anilines with acetic anhydride in water

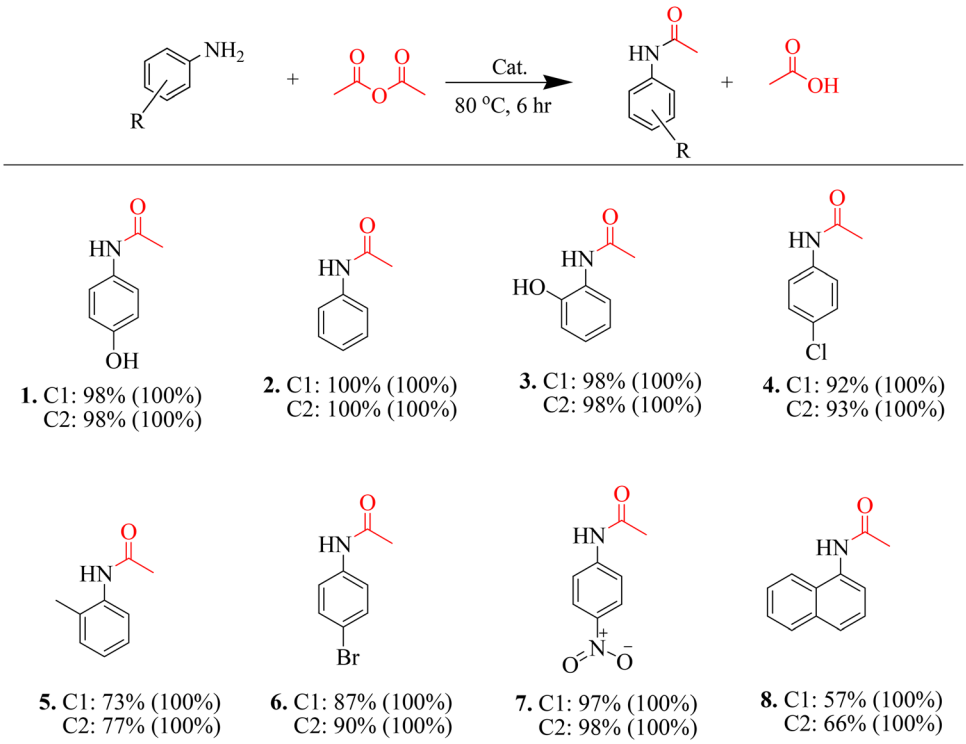

Results format: **Entry number** Yield (Selectivity)

C1 = catalyst 1 (5%WO_3-ZrO_2) C2 = catalyst 2 (5%MoO_3-SiO_2)

Reaction conditions: aniline (2 mmol), acetic anhydride (4 mmol), 5 mL 2 wt% HPMC solution, catalyst (50 mg), temperature (80 °C), time (6 h).

Table 3 The yields and selectivity of products formed by acetylation of selected primary and secondary amines with acetic anhydride in water

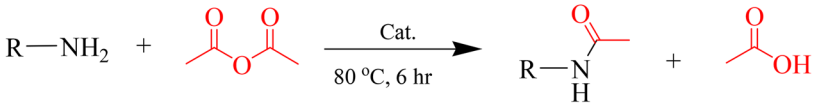

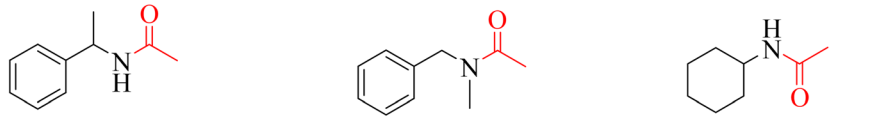

1. C1: 100% (100%)
C2: 100% (100%)

2. C1: 100% (100%)
C2: 98% (100%)

3. C1: 98% (100%)
C2: 98% (100%)

Results format: **Entry number** Yield (Selectivity)

C1 = catalyst 1 (5%WO_3-ZrO_2) C2 = catalyst 2 (5%MoO_3-SiO_2)

Reaction conditions: primary amine (2 mmol), acetic anhydride (4 mmol), 5 mL 2 wt% HPMC solution, catalyst (50 mg), temperature (80 °C), time (6 h).

Table 4 The yields and selectivity of products obtained from acetylation of selected alcohols with acetic anhydride in water

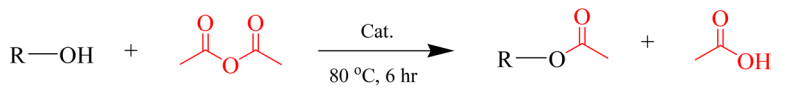

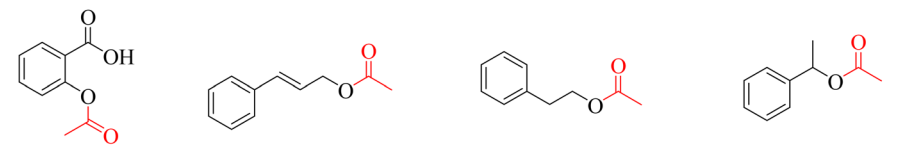

1. C1: 70% (100%)
C2: 78% (100%)

2. C1: 60% (100%)
C2: 27% (100%)

3. C1: 90% (100%)
C2: 65% (100%)

4. C1: 33% (100%)
C2: 27% (100%)

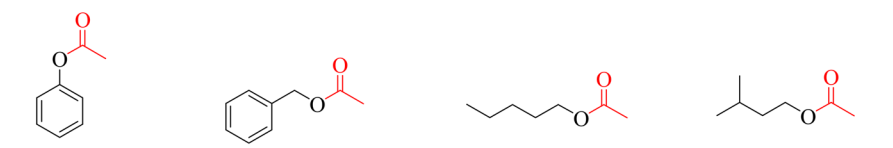

5. C1: 65% (100%)
C2: 46% (100%)

6. C1: 27% (100%)
C2: Trace

7. C1: 74% (100%)
C2: 59% (100%)

8. C1: 74% (100%)
C2: 55% (100%)

9. C1: 67% (100%)
C2: 54% (100%)

10. C1: 68% (100%)
C2: 57% (100%)

11. C1: 72% (100%)
C2: 68% (100%)

12. C1: 99% (100%)
C2: 50% (100%)

Results format: **Entry number** Yield (Selectivity)

C1 = catalyst 1 (5%WO_3-ZrO_2) C2 = catalyst 2 (5%MoO_3-SiO_2)

Reaction conditions: alcohol (2 mmol), acetic anhydride (4 mmol), 5 mL 2 wt% HPMC solution, catalyst (50 mg), temperature (80 °C), time (6 h).

acetaminophen, which has medicinal applications (used to treat fever and pain).[39] Secondly, this substrate has two functional groups that can be acetylated (OH and NH_2), making it a good model for determining selectivity for either functional group. The results show 100% selectivity for the amino group, with a 98% yield for both catalysts. There are no side products formed for this substrate, which makes this system highly efficient for synthesizing paracetamol, and thus potentially helpful for the pharmaceutical industry. Most of the other substrates also show high yields and selectivity, except for the one with an electron-donating methyl group substituent (entry 5), which exhibited moderate yields of less than 80%. The lower yield in the acetylation of 2-methylaniline compared to other substituted anilines is due to steric hindrance from the methyl group on 2-methylaniline, which obstructs the nucleophilic attack of the amine on the acetic anhydride's carbonyl carbon, making the reaction slower and incomplete. In addition, 1-naphthylamine substrate (entry 8) showed lower yields than 70%. The acetylation of 1-naphthylamine yields a lower quantity of product compared to anilines due to the greater steric hindrance around the amine group of 1-naphthylamine caused by the bulky fused ring system, which impedes the nucleophilic attack by acetic anhydride. Although the yields are quite close between the two catalysts, 5%WO_3–ZrO_2 and 5%MoO_3–SiO_2, labelled C1 and C2, respectively. The 5%MoO_3–SiO_2 seems to be slightly more effective in the acetylation of anilines.

3.2.2. Acetylation of amines. A few amines were also acetylated, and the evaluating results are reported in Table 3. Compared to anilines, amines are generally good nucleophiles because the lone pair of electrons on the nitrogen atom is more readily available for nucleophilic attack. However, in aniline, the lone pair on the nitrogen is delocalized into the pi system of the benzene ring which reduces their reactivity. Thus, the expectation was that the system would also be efficient for these substrates. Only one secondary amine was evaluated, and the yields and selectivity were 100% for 5%WO_3–ZrO_2 catalyst, and 98% and 100%, respectively for 5%MoO_3–SiO_2 catalyst (see Table 3).

3.2.3. Acetylation of alcohols. Based on the results in Table 2, especially the consideration for the paracetamol synthesis, *i.e.*, the system was selective for the amino group and formed the amide selectively instead of the ester. Alcohol is generally a weaker nucleophile than aniline. Alcohols, like aniline, have a lone pair of electrons on the oxygen atom and on the nitrogen atom, respectively, that can act as a nucleophile. However, the oxygen atom is highly electronegative, making it less likely to donate electrons to an electrophile compared to nitrogen. Thus, it would be difficult to obtain esters from the acetylation of alcohols, or at least the yields and conversions would be moderate. As expected, this was the general trend in most of the alcohols that were evaluated (see Table 4). In the reported mesoporous acid-catalysed acetylation of alcohols, the 5%WO_3–ZrO_2 catalyst is more active than the 5%MoO_3–SiO_2 catalyst, excepted for Entry 1. We could not detect the peaks for the aspirin on the GC-MS. However, we were able to isolate a yield of 78% (the NMR characterization is reported in the SI).

3.2.4. Performance of the catalysts and mechanistic pathways. Based on the results in Tables 2 to 4, it can be observed that, anilines and amines generally show higher reactivity than alcohols in the presence of both 5%WO_3–ZrO_2 and 5%MoO_3–SiO_2 catalysts. While both amines and alcohols can be acetylated, amines are generally more nucleophilic than alcohols, and the acetylation reaction mechanism differs slightly between them. Amines readily acetylate due to their higher nucleophilicity, while alcohols may require activation for efficient acetylation.[40,41] Thus, the higher nucleophilicity of the anilines and amines compared to alcohols justified the higher activity observed for both catalysts in these compounds with the HPMC/H_2O system.

Both catalysts demonstrated excellent reactivity and stability. The 5%MoO_3–SiO_2 catalyst was slightly more active in the acetylation of anilines, with conversions ranging from 76 to 100% (Table 2), while the 5%WO_3–ZrO_2 was more active in the acetylation of alcohols, with conversions ranging from 27 to 99% (Table 4). However, both catalysts were almost equally active in the acetylation of amines, with conversions of at least 98% and 100% selectivity (Table 3). The higher surface area of the 5%MoO_3–SiO_2 catalyst (97.07 $m^2\ g^{-1}$) compared to the 5%WO_3–ZrO_2 catalyst (62.33 $m^2\ g^{-1}$) appears to be the driving force for its better catalytic activity in the acetylation of anilines and amines. A larger surface area provides more active sites for the reaction to occur, increasing the reaction rate and potentially improving the yield of the acetylated product.[13,42] The mechanism of acetylation of anilines with acetic anhydride, catalyzed by MoO_3–SiO_2 in water, involves several steps, including: (i) nucleophilic attack, where the aniline's nitrogen lone pair attacks the electrophilic carbonyl carbon of acetic anhydride, forming a tetrahedral intermediate; (ii) leaving group departure, where the acetate ion leaves, taking electrons and forming a positively charged acylium ion; and (iii) rearrangement, where the nitrogen atom's lone pair migrates to the positively charged carbon, forming a new *N*-acetyl bond and completing the reaction. Scheme 1 illustrates the mechanistic pathway of the acetylation of anilines with acetic anhydride in water using MoO_3–SiO_2. The MoO_3 component of the catalyst acts as an acidic site, activating the carbonyl carbon of acetic anhydride by making it more electrophilic and thus facilitating the nucleophilic attack by anilines.[13] The aniline and acetic anhydride molecules adsorb onto the surface of the MoO_3–SiO_2 catalyst, bringing them into proximity and promoting the reaction. While water is used as the solvent, it does not directly participate in the reaction mechanism but may play a role in solvating the reactants and products.

In contrast, the acetylation of alcohols is more dependent on the acidity of the catalyst. Due to its high acidic content, 5%WO_3–ZrO_2 showed better catalytic activity compared to 5%MoO_3–SiO_2 in the acetylation of alcohols. The incorporation of WO_3 onto ZrO_2 enhances the surface acidity of the zirconia, providing active sites for the acid catalyzed acetylation. It is reported that the acid catalyst facilitate the reaction between an alcohol and an acetylating agent, typically acetic anhydride.[43,44] The WO_3–ZrO_2 catalyst itself then provides surface acidity,

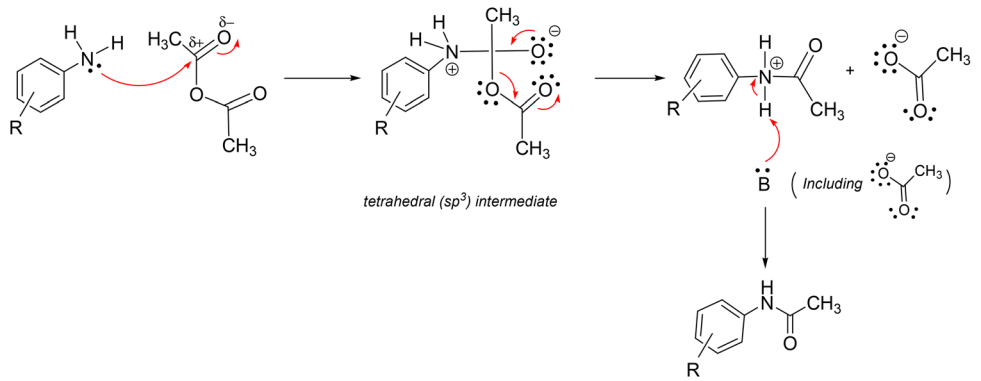

Scheme 1 The Proposed mechanism for the acetylation of anilines with acetic anhydride.

which is key to activating the acetic anhydride through a Lewis acid mechanism, making it more electrophilic and susceptible to nucleophilic attack. The proposed catalytic mechanism, which involves the acetylation of alcohols with acetic anhydride by WO_3–ZrO_2 in water, also consists of multiple steps, such as: (i) activation of acetic anhydride, which occurs when the acidic sites on the WO_3–ZrO_2 surface interact with the carbonyl oxygen atom of the acetic anhydride, polarizing it and making the carbonyl carbon more susceptible to nucleophilic attack; (ii) nucleophilic attack, where the alcohol, acting as a nucleophile, attacks the activated carbonyl carbon of the acetic anhydride; (iii) tetrahedral intermediate formation, where the carbon atom bonded to the alcohol oxygen is temporarily bonded to four groups; (iv) proton transfer, a proton is transferred from the alcohol's oxygen to a leaving group, such as an acetate ion. This proton transfer, potentially mediated by water or the acetate ion itself, results in the formation of the desired ester and acetic acid. Water in the reaction system acts as solvent, and as a reactant to regenerate the catalyst's active sites by facilitating the decomposition of intermediates. Thus, we postulated that the acetylation of alcohol in this study, is an acid surface-catalyst-driven reaction mechanism that leads to the formation of esters. Scheme 2 illustrates the mechanistic pathway of the acetylation of anilines with acetic anhydride in water using MoO_3–SiO_2.

3.2.5. Acyl source variation study. Table 5 shows the acyl source variation study that was done under mild conditions. The 5%WO_3–ZrO_2 catalyst was used for this study as its activity was generally high for the acetylation of all the different functional groups, especially in the case of alcohols, where the conversions were moderate. The conversions of the substrate (4-hydroxyaniline) were high, except for entry 1 (only 75%), where acetic acid was used as an acyl source. Another acylating agent in the form of ethyl acetoacetate was evaluated under various conditions. Under the reaction conditions investigated in this study (entry 4), the reaction was 100% selective to the desired product, and the conversion and yield were 100%. The reaction was also performed at room temperature without a catalyst, and with the addition of *tert*-butyl hydroperoxide (TBHP) as an oxidizing agent to radicalize the aldehyde (entry 5). The reaction appears to be spontaneous, with 100% conversion, yield, and selectivity. The effect of TBHP on the radicalisation of acyl sources in acylation was previously reported.[45,46] This reaction was repeated at room temperature, with no catalyst and without the addition of TBHP (entry 6). The reaction was reproducible, the conversion, yield, and selectivity were precisely the same, indicating that the reaction between 4-hydroxyaniline and ethyl acetoacetate in the HPMC/H_2O system is indeed spontaneous. The reaction mechanism consists of: (i) initial nucleophilic attack, where the amine of

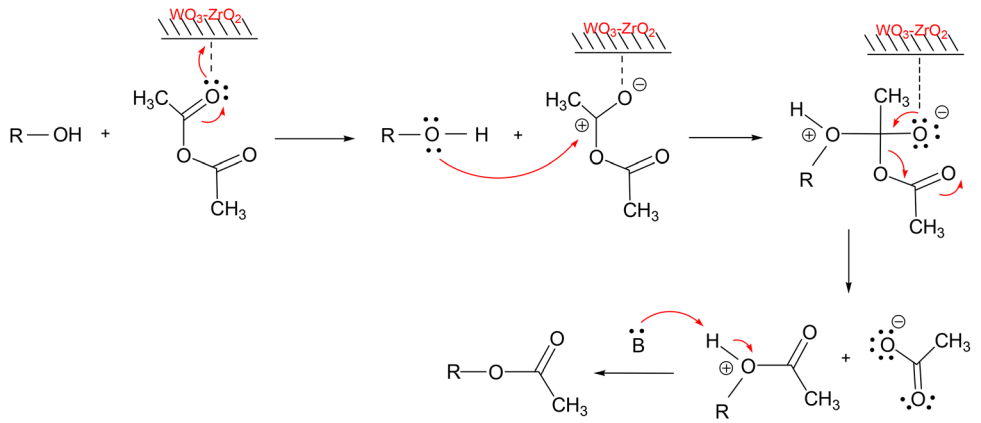

Scheme 2 The proposed mechanism for the acetylation of alcohols with acetic anhydride.

Table 5 The acylation of 4-hydroxyaniline using different acyl sources catalysed by 5%WO_3/ZrO_2

Entry	Acyl source	Conversion (%)	Yield (%)	Selectivity (%)	Major product
1	Acetic acid	75	70	100	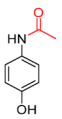
2	Formic acid	100	90	90	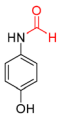
3	Vinyl acetate	100	100	100	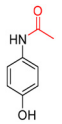
4	Ethyl acetoacetate	100	100	100	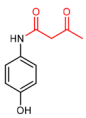
5	Ethyl acetoacetate[a]	100	100	100	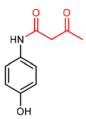
6	Ethyl acetoacetate[b]	100	100	100	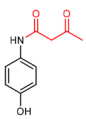

Reaction conditions: 4-Hydroxyaniline (2 mmol), Acyl source (2 equiv., 4 mmol), 5%WO_3/ZrO_2 (50 mg, 0.002 equiv.), 80 °C, 6 h. [a] *Tert*-Butyl hydroperoxide (2 equiv., 4 mmol), no catalyst, room temperature. [b] Without *tert*-Butyl hydroperoxide, no catalyst, room temperature.

4-hydroxyaniline attacks the carbonyl carbon of ethyl acetoacetate, forming an intermediate; (ii) condensation/elimination, where intermediate undergoes condensation and elimination of water and ethanol to form a substituted quinoline ring. The combination of a strong driving force (formation of a stable product) and the intrinsic reactivity of the reactants makes the reaction between 4-hydroxyaniline and ethyl acetoacetate a spontaneous one.

The formation of the products for acetylation using different acyl sources was further confirmed by ^{1}H NMR and ^{13}C NMR. The products and their corresponding spectra are presented in Fig. S2 and S3, respectively. The plausible structures of the products were matched from the GC software library, and a few GC–MS spectra are displayed in Fig. S4.

3.2.6. Comparison with literature. Table 6 presents the comparison of efficiencies for the different protocols for the acetylation of different substrates. For the paracetamol synthesis, the system used in this study (entry 1) is much more efficient (100% yield) compared to the protocol reported by Ghosh *et al.*[47] (entry 2; 75% yield), which uses toluene as solvent at high temperature, and with no catalyst. The protocol by Farhadi *et al.*[48] (entry 3) utilizes a $ZnAl_2O_4$@SiO_2 nanocomposite under solvent-free conditions and at a slightly lower temperature, showing a comparable result (95% yield) with our HPMC/H_2O system. The acetylation of secondary and primary amines, namely *N*-methylbenzylamine and α-methylbenzylamine, in our HPMC/H_2O system (entries 4 and 6; 100% yield) is more efficient compared to the protocols respectively reported by Sharley *et al.*[38] (entry 5) and Ghosh *et al.*[47] (entry 7). Both protocols are at higher temperatures and make use of organic solvents with lower yields, 91% and 96%, respectively. In terms of the acetylation of alcohols, the substrate 2-phenylethanol, using the most acidic catalyst in this study, had the highest conversion. Compared to the protocols by Farhadi *et al.*[48] (entry 9) and Basumatary *et al.*[49] (entry 10), which both operate at a slightly lower temperature, our catalytic system (entry 8) proved to be rather comparable.

Although different reaction conditions were used, in general, the performances of the catalysts studied in our systems were comparable to or even better than other catalysts. Our catalytic systems show better results under mild and green reaction conditions. The better results obtained for our catalytic system can be attributed to the acid nature of the as-prepared catalysts and the high active catalytic site density. Several studies have reported that Acetylation reactions can be mediated by acid catalysts to activate an acylating agent, such as acetic anhydride.[4,5,50] The acid catalyst protonates the carbonyl oxygen of the acetic anhydride, making the carbonyl carbon more electrophilic and susceptible to attack by the nucleophile, such as anilines, amines, or alcohols.[40,43,50–52]

Table 6 Comparison of the efficiency of 5%WO_3–ZrO_2 in the 2 wt.% HPMC protocol with other protocols for the acetylation of 4-hydroxyaniline, *N*-methylbenzylamine, α-methylbenzylamine, and 2-phenylethanol

Entry	Substrate	Catalyst	Solvent	Temp. (°C)	Yield (%)	Ref.
1	4-Hydroxyaniline	5%WO_3/ZrO_2	HPMC/H_2O	80	100	TW
2	4-Hydroxyaniline	—	Toluene	Reflux	75	47
3	4-Hydroxyaniline	$ZnAl_2O_4$@SiO_2	—	75	95	48
4	*N*-methylbenzylamine	5%WO_3/ZrO_2	HPMC/H_2O	80	100	TW
5	*N*-methylbenzylamine	Acetic acid	Butyl acetate	120	91	38
6	α-methylbenzylamine	5%WO_3/ZrO_2	HPMC/H_2O	80	100	TW
7	α-methylbenzylamine	—	Toluene	Reflux	96	47
8	2-Phenylethanol	5%WO_3/ZrO_2	HPMC/H_2O	80	90	TW
9	2-Phenylethanol	$ZnAl_2O_4$@SiO_2	—	75	92	48
10	2-Phenylethanol	I_2	Ethyl acetate	Reflux	95	49

TW = This work.

3.3. Catalyst reusability

The reaction between aniline and acetic anhydride catalysed by 5%WO_3–ZrO_2 was used for recyclability studies and was scaled up by a factor of two. As a result, 100 mg of the most active catalyst, 5%WO_3–ZrO_2 was used. Fig. 6 shows the results of the catalyst recycle tests, which indicate the stability of the as-synthetized catalyst, as up to a fifth cycle, the conversion remained the same, 100%. However, the catalyst becomes a lump after the fourth run and cannot be pulverized after drying. Although the formation of the lump and the subsequent reduction in surface area, the catalyst was still highly active with a 100% conversion. Generally, a catalyst becomes a lump after recycling because it undergoes deactivation and agglomeration, a process where the active sites on the catalyst surface become blocked or altered, causing particles to clump together, leading to reduced activity. This can happen due to coking (carbonaceous deposits form on the catalyst surface), poisoning (contaminants in the feed stream binding strongly to the catalyst's active sites), sintering (high operating temperatures causing small catalyst particles to fuse together), or leaching (the active material dissolving or washing away into the reaction mixture).[53,54] To prevent lump formation, several methods can be employed, including regeneration techniques involving various chemical or thermal treatments (*e.g.* washing, calcination, or dissolution of deposited materials from the catalyst surface), optimized recycling processes, to separate and recover the active catalyst material effectively by minimizing damage during recovery, and designing catalysts with enhanced structural stability and resistance to lumps formation and deactivation.[54] However, a catalyst can form a lump without losing its activity, as is the case in this study. The overall structure of the catalyst can remain intact, such as a solid bulk catalyst, while its surface or internal structure provides the active sites where the chemical transformation occurs. The catalytic activity comes from specific active sites on the surface of the catalyst or within its pores, where reactant molecules adsorb onto, undergo transformation, and then desorb as products.[53] Twenty percent of the catalyst was lost after the fifth cycle during workup between the different cycles. However, the conversion was still maximum. This indicated that the catalyst could be reused several times under our catalytic system without significant loss in activity. It can also be observed in Fig. 7(a) that there is no substantial change in the 5%WO_3–ZrO_2 structure after fifth run. The original peaks are still visible, which means the crystalline structure of the materials is preserved. Also, Fig. (7b) shows that the surface morphology of the catalysts did not significantly change after the fifth run, again demonstrating the catalyst's stability. These features make it a good catalyst for academic research as well as industrial application.

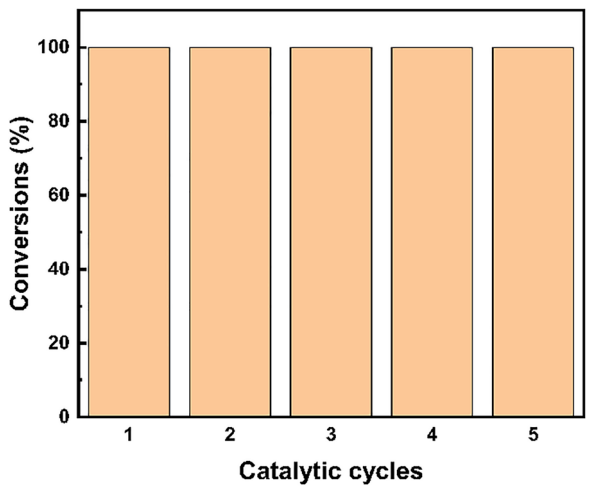

Fig. 6 The catalytic recycle test of 5%WO_3–ZrO_2. Conditions: aniline (4 mmol), acetic anhydride (2 equiv., 8 mmol), 5%WO_3/ZrO_2 (100 mg, 0.002 equiv.) at 80 °C for 6 h.

4. Conclusions

In this study, highly stable doped mesoporous metal oxides were successfully synthesized using a sol–gel method. We successfully demonstrated the acetylation of anilines, amines and alcohols in the HPMC/H_2O system. We also showed that the 5%MoO_3–SiO_2 and 5%WO_3–ZrO_2 acid catalysts are water stable, highly active for acetylation, and reusable. In most cases, the conversions, yields and selectivity were high, with

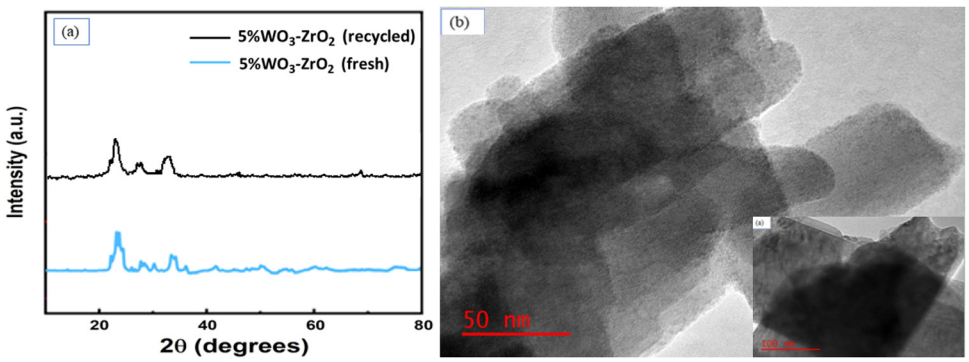

Fig. 7 (a) Wide-angle p-XRD patterns of recycled and fresh 5%WO_3–ZrO_2; (b) TEM image of recycled 5%WO_3–ZrO_2, and a thumbnail of a fresh 5%WO_3–ZrO_2.

the added advantage that we used a solvent system that is biodegradable and environmentally benign at relatively mild reaction conditions. This protocol aligns to the Green Chemistry requirements and offers an advantage over other approaches. These alternative methods often require high temperatures or utilize solvents that are damaging to the environment, making our approach a more sustainable and effective solution.

Conflicts of interest

The authors declare no conflict of interest.

Data availability

All data reported in this work are available from the supplementary information (SI). Supplementary information: conversion percentage, selectivity percentage, and GC Yield percentage (eqn (S1)–(S3)), NH_3-TPD profiles of the catalysts (Fig. S1); ^1H NMR and ^{13}C NMR of acetylation products (Fig. S2); NMR spectra of the products of acetylation (Fig. S3); The GC-MS spectra of the plausible products obtain during acetylation (Fig. S4). See DOI: **https://doi.org/10.1039/d5nj02857d**.

Acknowledgements

This work is based on the research supported in part by the National Research Foundation of South Africa (Grant number BCSA210302588432). We would like also to thank the University of Johannesburg for funding, and Shimadzu South Africa, for the use of their equipment. We acknowledge Ms EC. Kassim for language editing the manuscript.

References

1 G. Sartori, R. Ballini, F. Bigi, G. Bosica, R. Maggi and P. Righi, *Chem. Rev.*, 2004, **104**, 199–250.
2 P. Hodge, *Polymer*, 1992, **33**, 3542.
3 B. Karimi and J. Maleki, *J. Org. Chem.*, 2003, **68**, 4951–4954.
4 M. Seddighi, F. Shirini and O. Goli-Jolodar, *Comptes Rendus Chim.*, 2016, **19**, 1003–1010.
5 K. Niknam and D. Saberi, *Tetrahedron Lett.*, 2009, **50**, 5210–5214.
6 R. M. Lanigan and T. D. Sheppard, *Eur. J. Org. Chem.*, 2013, 7453–7465.
7 L. Mrózek, L. Dvořáková, Z. Mandelová, L. Rárová, A. Řezáčová, L. Plaček, R. Opatřilová, J. Dohnal, O. Paleta and V. Král, *Steroids*, 2011, **76**, 1082–1097.
8 B. Schilter, G. Scholz and W. Seefelder, *Eur. J. Lipid Sci. Technol.*, 2011, **113**, 309–313.
9 R. Nagase, N. Matsumoto, K. Hosomi, T. Higashi, S. Funakoshi, T. Misaki and Y. Tanabe, *Org. Biomol. Chem.*, 2007, **5**, 151–159.
10 A. Zoller and A. Marcilla, *J. Appl. Polym. Sci.*, 2011, **121**, 1495–1505.
11 S. Farhadi and S. Panahandehjoo, *Appl. Catal., A*, 2010, **382**, 293–302.
12 E. Rezaei-Seresht, F. M. Zonoz, M. Estiri and R. Tayebee, *Ind. Eng. Chem. Res.*, 2011, **50**, 1837–1846.
13 X. S. Hlatshwayo, M. J. Ndolomingo, N. Bingwa and R. Meijboom, *RSC Adv.*, 2021, **11**, 16468–16477.
14 X. S. Hlatshwayo, M. S. Xaba, M. J. Ndolomingo, N. Bingwa and R. Meijboom, *Catalysts*, 2021, **11**, 673.
15 B. H. Lipshutz, *J. Org. Chem.*, 2017, **82**, 2806–2816.
16 A. Chanda and V. V. Fokin, *Chem. Rev.*, 2009, **109**, 725–748.
17 G. Cravotto, E. Borretto, M. Oliverio, A. Procopio and A. Penoni, *Catal. Commun.*, 2015, **63**, 2–9.
18 D. Petkova, N. Borlinghaus, S. Sharma, J. Kaschel, T. Lindner, J. Klee, A. Jolit, V. Haller, S. Heitz, K. Britze and J. Dietrich, *ACS Sustainable Chem. Eng.*, 2020, **8**, 12612–12617.
19 W. Braje, K. Britze, J. D. Dietrich, A. Jolit, J. Kaschel, J. Klee and T. Lindner, *U.S. Pat. Appl.*, 2017, **15/417**, 806.
20 M. Cortes-Clerget, J. Yu, J. R. Kincaid, P. Walde, F. Gallou and B. H. Lipshutz, *Chem. Sci.*, 2021, **12**, 4237–4266.
21 N. Borlinghaus, V. Wittmann and W. M. Braje, *Curr. Opin. Green Sustain. Chem.*, 2022, **33**, 100571.
22 J. Xu, A. Zheng, J. Yang, Y. Su, J. Wang and D. Zeng, *J. Phys. Chem. B*, 2006, **110**, 10662–10671.
23 R. G. Pearson and J. Songstad, *J. Am. Chem. Soc.*, 1967, **39**, 1827–1836.
24 N. Masunga, G. S. Tito and R. Meijboom, *Appl. Catal., A*, 2018, **552**, 154–167.
25 M. V. Kovalenko, Y. M. Romanenko, T. O. Soloviova and P. I. Loboda, *Powder Metall. Met. Ceram.*, 2023, **61**, 541–547.
26 I. M. S. Anekwe, B. Oboirien and Y. M. Isa, *Fuel Commun.*, 2024, **18**, 100101.
27 C. Lin, K. Tao, H. Yu, D. Hua and S. Zhou, *Catal. Sci. Technol.*, 2014, **4**, 4010–4019.
28 C. A. Akinnawo, N. Bingwa and R. Meijboom, *Catal. Commun.*, 2020, **145**, 106115.
29 M. A. Cortes-Jacome, J. A. Toledo-Antonio, H. Armendáriz, I. Hernández, X. Bokhimi and J. Solid, *State Chem.*, 2002, **164**, 339–344.
30 R. Kourieh, S. Bennici, M. Marzo, A. Gervasini and A. Auroux, *Catal. Commun.*, 2012, **19**, 119–126.
31 A. Martínez, G. Prieto, M. A. Arribas, P. Concepción and J. F. Sánchez-Royo, *J. Catal.*, 2007, **248**, 288–302.
32 A. S. Poyraz, C. H. Kuo, E. Kim, Y. Meng, M. S. Seraji and S. L. Suib, *Chem. Mater.*, 2014, **26**, 2803.
33 A. Corma, *Chem. Rev.*, 1997, **97**, 2373–2420.
34 S. Royer, D. Duprez, F. Can, X. Courtois, C. Batiot-Dupeyrat, S. Laassiri and H. Alamdari, *Chem. Rev.*, 2014, **114**, 10292–10368.
35 S. K. Vishwanath, T. An, W. Y. Jin, J. W. Kang and J. Kim, *J. Mater. Chem. C*, 2017, **5**, 10295–10301.
36 J. H. Merino, J. Bernad and X. Solans-Monfort, *Top. Catal.*, 2022, **65**, 433–447.
37 M. V. Zakharova, F. Kleitz and F. G. Fontaine, *Dalton Trans.*, 2017, **46**, 3864–3876.
38 D. D. Sanz Sharley and J. M. J. Williams, *Chem. Commun.*, 2017, **53**, 2020–2023.

39 S. N. Mane, S. M. Gadalkar and V. K. Rathod, *Ultrason. Sonochem.*, 2018, **49**, 106–110.
40 N. Anbu, N. Nagarjun, M. Jacob, J. M. V. K. Kalaiarasi and A. Dhakshinamoorthy, *Chem.*, 2019, **1**, 69–79.
41 H. Inoue, T. Tachibana, T. Bito and J. Arima, *Enzyme Microb. Technol.*, 2023, **165**, 110208.
42 A. E. A. Said and M. M. Abd El-Wahab, *J. Chem. Tech. Biotechnol.*, 2006, **81**, 329–335.
43 C. Liu, S. J. Li, P. Han, L. B. Qu and Y. Lan, *Mol. Catal.*, 2021, **499**, 111318.
44 A. Mannu and A. Mele, *Catalysts*, 2024, **14**, 931.
45 A. Gupta, A. Kherudkar and J. K. Laha, *J. Org. Chem.*, 2025, **90**, 6392–6406.
46 R. Boora and B. S. Reddy, *Org. Biomol. Chem.*, 2019, **17**, 9627–9630.
47 S. Ghosh, A. Purkait and C. K. Jana, *Green Chem.*, 2020, **22**, 8721–8727.
48 S. Farhadi and K. Jahanara, *Chin. J. Catal.*, 2014, **35**, 368–375.
49 G. Basumatary and G. Bez, *Tetrahedron Lett.*, 2017, **58**, 4312–4315.
50 M. M. Heravi, F. K. Behbahani and F. F. Bamoharram, *J. Mol. Catal. A: Chem.*, 2006, **253**, 16–19.
51 M. Akçay, *Appl. Catal., A*, 2004, **269**, 157–160.
52 I. Jain, R. Sharma and P. Malik, *Synth. Commun.*, 2019, **49**, 2952–2960.
53 R. Quintana-Solórzano, A. Rodríguez-Hernández and R. García-de-León, *Ind. Eng. Chem. Res.*, 2009, **48**, 1163–1171.
54 Á. Molnár and A. Papp, *Coord. Chem. Rev.*, 2017, **349**, 1–65.

